Effects of electron irradiation on resistivity and London penetration depth of $Ba_{1-x}K_{x}Fe_{2}As_{2}$ ($x \leq 0.34$) iron-pnictide superconductor

K. Cho, M. Kończykowski, J. Murphy, H. Kim, M. A. Tanatar, W. E. Straszheim, B. Shen, H. H. Wen, and R. Prozorov

Phys. Rev. B **90**, 104514 — Published 19 September 2014

DOI: 10.1103/PhysRevB.90.104514

Effects of electron irradiation on resistivity and London penetration depth of $Ba_{1-x}K_xFe_2As_2$ ($x \leq 0.34$) iron-pnictide superconductor

K. Cho,[1] M. Kończykowski,[2] J. Murphy,[1] H. Kim,[1] M. A. Tanatar,[1]
W. E. Straszheim,[1] B. Shen,[3] H. H. Wen,[3] and R. Prozorov[1,*]

[1] *The Ames Laboratory and Department of Physics & Astronomy, Iowa State University, Ames, IA 50011, USA*
[2] *Laboratoire des Solides Irradiés, CNRS UMR 7642 & CEA-DSM-IRAMIS, Ecole Polytechnique, F-91128 Palaiseau cedex, France*
[3] *Center for Superconducting Physics and Materials, National Laboratory of Solid State Microstructures & Department of Physics, Nanjing University, Nanjing 210093, China*

(Dated: 28 July 2014)

Irradiation with 2.5 MeV electrons at doses up to 5.2 $\times 10^{19}$ electrons/cm^2 was used to introduce point-like defects in single crystals of $Ba_{1-x}K_xFe_2As_2$ with $x = 0.19$ ($T_c = 14$ K), 0.26 ($T_c = 32$ K), 0.32 ($T_c = 37$ K), and 0.34 ($T_c = 39$ K) to study the superconducting gap structure by probing the effect of non-magnetic scattering on electrical resistivity, $\rho(T)$, and London penetration depth, $\lambda(T)$. For all compositions, the irradiation suppressed the superconducting transition temperature, T_c and increased resistivity. The low-temperature behavior of $\lambda(T)$ is best described by the power-law function, $\Delta\lambda(T) = A(T/T_c)^n$. While substantial suppression of T_c supports $s_\pm$ pairing, in samples close to the optimal doping, $x = 0.26$, 0.32, and 0.34, the exponent n remained high ($n \geq 3$) indicating almost exponential attenuation, thus robust full superconducting gap. For the $x = 0.19$ composition that exhibits coexistence of superconductivity and long-range magnetism, the suppression of T_c was much more rapid and the exponent n decreased toward $s_\pm$ dirty limit of $n = 2$. In this sample, the irradiation also suppressed the temperature of structural/magnetic transition, T_{sm}, from 103 K to 98 K consistent with the itinerant nature of the long-range magnetic order. Our results suggest that under-doped compositions, especially in the coexisting regime are most susceptible to non-magnetic scattering and imply that in multi-band $Ba_{1-x}K_xFe_2As_2$ superconductors, the ratio of the inter-band to intra-band pairing strength, as well as the related gap anisotropy, increases upon the departure from the optimal doping.

PACS numbers: 74.70.Xa,74.20.Rp,74.62.Dh

I. INTRODUCTION

Studying the effects of controlled point-like disorder on superconducting properties is a powerful tool to understand the mechanisms of superconductivity[1–8]. According to the Anderson's theorem, conventional isotropic $s-$wave superconductors are not affected by the potential (non-magnetic) scattering, but are sensitive to a spin-flip scattering on magnetic impurities[1]. In high$-T_c$ cuprates, both magnetic and non-magnetic impurities cause rapid suppression of the superconducting transition temperature, T_c, strongly supporting $d-$wave pairing[9]. Similarly, for an order parameter changing sign between the sheets of the Fermi surface ($s_\pm$ pairing), considered the most plausible in multi-band iron-based superconductors (FeSCs)[10–12], the response to non-magnetic scattering is expected to be significant[12,13]. We should note that the multi-band character of superconductivity itself does not lead to the anomalous response to non-magnetic disorder beyond expected smearing of the gap variation on the Fermi surface, including the difference in gap magnitudes between the different bands[14]. For example, in a known two-gap s_{++} superconductor, MgB_2, electron irradiation resulted only in a minor change in T_c[15]. The sign change of the order parameter either along one sheet of the Fermi surface or between the sheets is what causes the dramatic suppression of T_c due to pair-breaking nature of inter-band scattering in this case.

A relatively slow rate of T_c suppression with disorder found in several experiments in iron-based superconductors was used as an argument for the s_{++} pairing, expected in orbital fluctuations - mediated superconductivity[16,17]. In reality, the situation in sign-changing multi-band superconductors is more complicated due to the competition between intra-band and inter-band pairing and, also, band-dependent scattering times and gap anisotropies[6,11,12]. Realistic calculations of the effect of point-like disorder on T_c within $s_\pm$ scenario[6] agree very well with the experiment, for example in electron irradiated $Ba(Fe_{1-x}Ru_x)_2As_2$[7] and $BaFe_2(As_{1-x}P_x)_2$[8].

Experimentally, it is quite difficult to introduce controlled point-like disorder. Studies of the disorder introduced by chemical substitution[18–20], heavy-ion or particle irradiation produced results that differ significantly from each other as far as the impact on the superconducting and materials properties is concerned[21–26]. Chemical substitution changes both crystalline and electronic structure and most particle irradiations introduce correlated disorder, in forms of columnar defects and/or clusters of different spatial extent[27]. The effective scattering potential strength and range (size) of such defects is very different from point-like scattering. On the other hand, MeV - range electron irradiation is known to produce va-

cancy/interstitial (Frenkel) pairs, which act as efficient point-like scattering centers[27]. This is consistent with the analysis of the collective pinning in $BaFe_2(As_{1-x}P_x)_2$ and $Ba(Fe_{1-x}Co_x)_2As_2$[28] as well as penetration depth in $BaFe_2(As_{1-x}P_x)_2$[8]. In the high-T_c cuprates, electron irradiation defects are known to be strong unitary scatterers causing significant suppression of T_c[29].

In addition to T_c, another parameter sensitive to disorder is quasi-particle density, which may be probed, for example, by measuring London penetration depth, $\lambda(T)$. In the case of isotropic single band $s-$wave or multiband $s_{++}-$wave superconductors, $\lambda(T)$ remains exponential at low temperatures with the addition of nonmagnetic scattering[6,13,30], whereas in the case of nodeless $s_{\pm}$ pairing it changes from exponential in the clean limit to $\sim T^2$ in the dirty limit[6,13]. Yet, an opposite behavior is observed in superconductors with line nodes where $\lambda \sim T$ in the clean limit changing to $\sim T^2$ in the dirty limit[3,31–33]. In the case of pnictide superconductors with accidental nodes, $\lambda(T)$ evolves from linear to exponential and, ultimately, to the T^2 behavior[8]. The details of the evolution from clean to dirty limit also depend on the (usually unknown) scattering potential amplitude and spatial extent. Weak Born scattering approximation, usually valid for normal metals, could not explain the rapid $T \rightarrow T^2$ evolution in the cuprates, so the unitary limit was used instead[4,33]. In iron-based superconductors, the situation is unclear and it seems that intermediate scattering amplitudes (modeled within $T-$matrix approach) are needed[6,7,13]. The spatial extent of the scattering potential affects the predominant scattering Q-vector, and it was suggested as the cause of a notable difference in quasi-particle response and evolution of T_c in $SrFe_2(As_{1-x}P_x)_2$ with natural and artificial disorder[34].

In this paper, we study the effects of electron irradiation on superconducting T_c and quasi-particle excitations of hole-doped $(Ba_{1-x}K_x)Fe_2As_2$ single crystals by measuring in-plane resistivity, $\rho(T)$, and in-plane London penetration depth, $\Delta\lambda(T)$. $(Ba_{1-x}K_x)Fe_2As_2$ has the highest $T_c \approx 40$ K among the 122 family and at the optimal doping reveals extremely robust superconductivity[25,35,36]. The superconducting gap structure of $(Ba_{1-x}K_x)Fe_2As_2$ varies with composition from full isotropic gap at the optimal doping to the gap with line nodes at $x = 1$[37–39]. On the under-doped side of interest here, gap anisotropy increases towards the edge of the superconducting dome, especially in the range of bulk coexistence of superconductivity and long range magnetic order[36,40]. This might imply that the ratio of the inter-band to intra-band pairing, as well as gap anisotropy, increase upon the departure from the optimal doping.

II. EXPERIMENTAL

Single crystals of $(Ba_{1-x}K_x)Fe_2As_2$ were synthesized using high temperature FeAs flux method[42]. Samples used in this study were cleaved from the inner parts of single crystals and were first extensively characterized using radio-frequency magnetic susceptibility as well as magneto-optical imaging to exclude chemical and spatial inhomogeneity. The compositions of $x = 0.19$, 0.26, and 0.34 were measured from wavelength dispersive spectroscopy (WDS) technique except for $x = 0.32$ where its composition was estimated from comparison with a T_c - x phase diagram in Ref. [41]. Four-probe measurements of in-plane resistivity were performed in *Quantum Design* PPMS. Samples for resistivity measurements had typical dimensions of (1-2)×0.5×(0.02-0.1) mm^3. Electrical contacts to samples prior to irradiation were made by soldering 50 μm silver wires with ultra-pure tin solder, as described in Ref. [43]. The in-plane London penetration depth, $\Delta\lambda(T)$, was measured using a self-oscillating tunnel-diode resonator technique[44,45]. The samples had typical dimensions of 0.5×0.5×0.03 mm^3. Details of the measurements and calibration can be found elsewhere[44]. The 2.5 MeV electron irradiation was performed at the SIRIUS Pelletron facility of the *Laboratoire des Solides Irradiés (LSI)* at the *École Polytechnique* in Palaiseau, France[28]. The acquired irradiation dose is conveniently measured in C/cm^2, where 1 C/cm^2 = 6.24 ×10^{18} electrons/cm^2. The details of the measurements and doses of electron irradiation are summarized in Table I. London penetration depths in samples 0.26-B and 0.34-B were measured in the same samples before and after the irradiation. For these samples, resistivity after electron irradiation was measured by gluing the contacts with silver paint to prevent defect annealing during sol-

TABLE I. List of samples measured before and after electron irradiation. 1 C/cm^2 = 6.24 ×10^{18} electrons/cm^2. WDS was conducted for $x = 0.19$, 0.26, and 0.34 samples. For $x = 0.32$ sample, x was estimated comparing its T_c with a T_c - x phase diagram in Ref. [41].

x	sample label	measurement
0.19	0.19-A	ρ before irradiation
	0.19-A	ρ after 1.8 C/cm^2 irradiation
	0.19-A	$\Delta\lambda$ after 1.8 C/cm^2 irradiation
	0.19-B	$\Delta\lambda$ before irradiation
0.26	0.26-A	ρ before irradiation
	0.26-B	$\Delta\lambda$ before irradiation
	0.26-B	$\Delta\lambda$ after 1.5 C/cm^2 irradiation
	0.26-B	ρ after 1.5 C/cm^2 irradiation
	0.26-B	$\Delta\lambda$ after 1.5 + 1.1 C/cm^2 irradiation
0.32	0.32-A	$\Delta\lambda$ before irradiation
	0.32-A	$\Delta\lambda$ after 8.3 C/cm^2 irradiation
0.34	0.34-A	ρ before irradiation
	0.34-B	$\Delta\lambda$ before irradiation
	0.34-B	$\Delta\lambda$ after 2.0 C/cm^2 irradiation
	0.34-B	ρ after 2.0 C/cm^2 irradiation

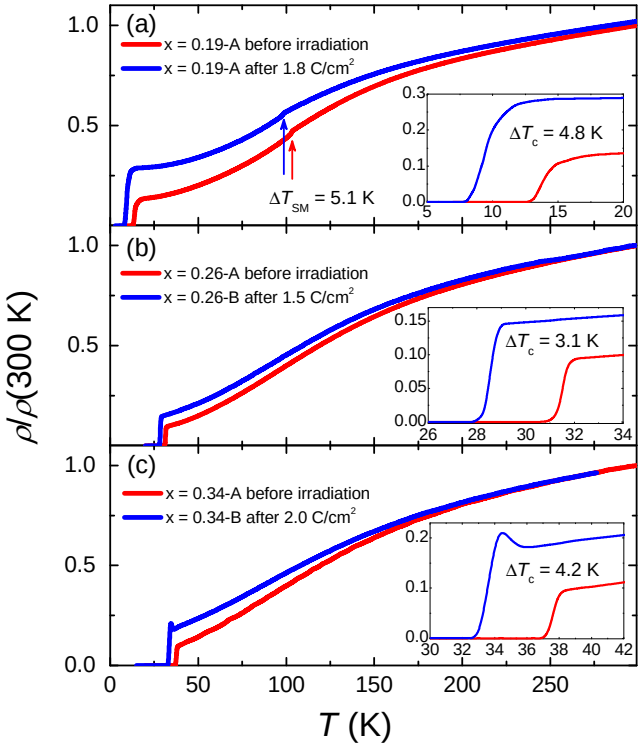

FIG. 1. (Color online) Temperature dependent resistivity normalized by the value at 300 K upon electron irradiation: (a) $x = 0.19$-A, (b) $x = 0.26$-A and B, and (c) $x = 0.34$-A and B. Insets zoom on the superconducting transitions.

dering process. (This, of course, is not the optimal technique, but otherwise the induced defects could be annealed by the soldering). The samples 0.26-A and -B for resistivity were cut from the same large slab and the same was done for the 0.34-A and -B ones. For $x = 0.19$, the 0.19-A sample was prepared for resistivity measurements with soldered contacts. Its temperature-dependent resistivity was measured in pristine and irradiated states, see Fig. 1 (a). Afterward, the contacts were removed to measure London penetration depth.

III. RESULTS AND DISCUSSION

Figure 1 shows normalized in-plane resistivity, $\rho(T)/\rho(300K)$, measured before and after electron irradiation in samples with (a) $x = 0.19$, (b) $x = 0.26$ and (c) $x = 0.34$. Insets zoom on superconducting transitions. For samples of all three doping levels, the introduction of disorder leads to a notable increase of residual resistivity. Superconducting transition temperature, T_c, was determined by linear extrapolation of $\rho(T)$ at the transition to $\rho = 0$. Overall, the irradiation doses of 1.5 to 2.0 C/cm^2 lead to T_c decrease by 3 to 5 K, see Fig. 4. Samples with $x = 0.26$ and $x = 0.34$ were outside the range of the coexisting magnetism and superconductivity. For $x = 0.19$, in addition to superconductivity, the

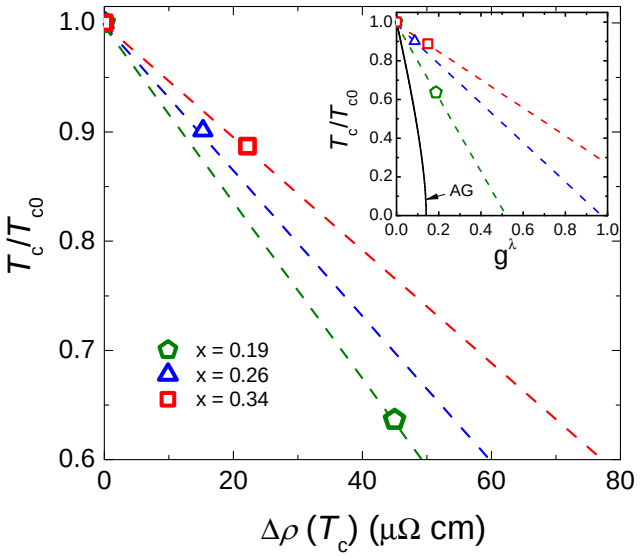

FIG. 2. (Color online) Experimental data of T_c/T_{c0} versus $\Delta\rho(T_c)$ upon electron irradiation, where $\rho(T_c)$ is the resistivity right above T_c and $\Delta\rho(T_c)$ is the change of the resistivity after irradiation. Inset shows T_c/T_{c0} versus dimensionless scattering rate g^λ. The classical Abrikosov-Gor'kov (AG) theory for an isotropic $s-$wave superconductor with magnetic impurities is also shown by a solid line[2].

long-range magnetic order develops simultaneously with orthorhombic distortion below structural/magnetic transition, T_{sm}. This transition is revealed as a small feature in $\rho(T)$ marked with the up-arrows in Fig. 1 (a). The T_{sm} before irradiation was about 103 K consistent with the previous report[46]. Irradiation with 1.8 C/cm^2 leads to T_{sm} decrease by 5.1 K, supporting the itinerant nature of antiferromagnetism[47]. A "bump" in $\rho(T)$ above T_c developed after the irradiation in the sample with $x = 0.34$, similar to electron irradiated YBaCuO, where it was interpreted to be due to localization effects[29]. However, more likely this feature in an artifact resulted from high and temperature - dependent contact resistance. The sample 0.34-B was small since, initially used for penetration depth measurement. To measure resistivity, the contacts were glued on later.

Figure 2 shows the variation of T_c/T_{c0} versus $\Delta\rho(T_c)$. From these values, we estimated the dimensionless scattering rate (g^λ) defined in a simple form as[7,48],

$$g^\lambda = \frac{\hbar}{2\pi k_B \mu_0} \frac{\Delta\rho(T_c)}{T_{c0}\lambda(0)^2} \qquad (1)$$

where $\Delta\rho(T_c)$ is the change in resistivity at T_c after the irradiation. Zero-temperature London penetration depth, $\lambda(0)$, was estimated from the Homes scaling[49], which takes into account both, the doping dependence and the change with pair-breaking scattering[33], see Fig. 4 and the corresponding text. The g^λ estimated from equation (1) was plotted in the inset of Fig. 2. The largest variation of $d(T_c/T_{c0})/dg^\lambda = -1.94$ was obtained for $x = 0.19$

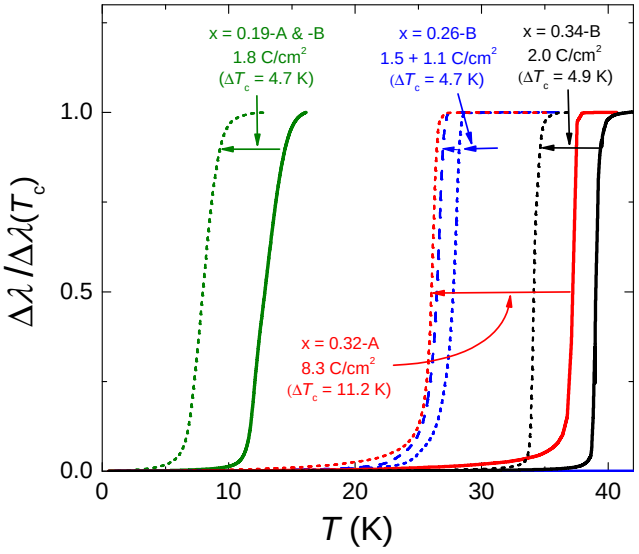

FIG. 3. (Color online) Variation of normalized in-plane penetration depth, $\Delta\lambda(T)/\Delta\lambda(T_c)$, before and after electron irradiation, see Table I for the details of the samples.

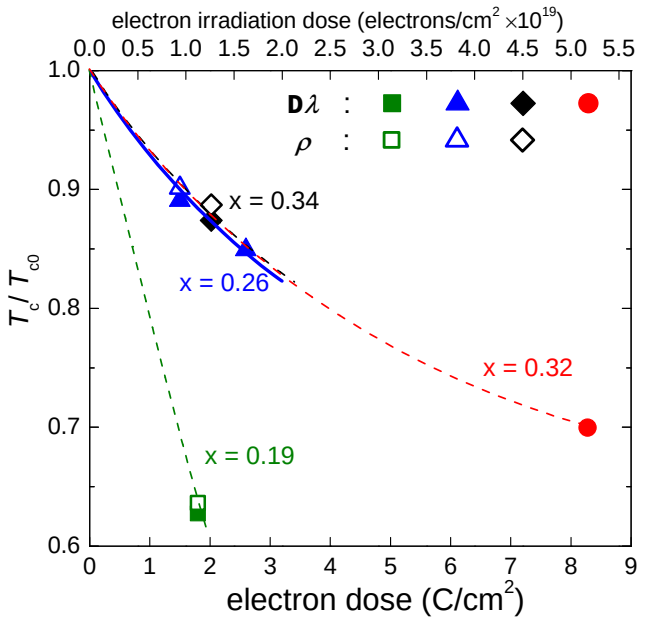

FIG. 4. (Color online) Variation of the reduced critical temperature, T_c/T_{c0}, with the dose of electron irradiation for samples $x = 0.19$ (green squares), $x = 0.26$ (blue triangles), $x = 0.26$ (black diamonds) and $x = 0.34$ (red circles).

while the smallest change of $d(T_c/T_{c0})/dg^{\lambda}$ = - 0.76 for $x = 0.34$. This indicates that the electron irradiation is more efficient for under-doped compounds which have a fragile superconductivity competing with long-range magnetism.

Figure 3 shows the normalized variation of the London penetration depth, $\Delta\lambda(T)$, measured down to $\sim$ 450 mK before and after electron irradiation for all three compositions. Magnetic superconducting transition temperature, T_c, was defined at a point of 50% of the total change at the phase transition and was consistent with the transport measurements shown in Fig. 1. The superconducting phase transition remained sharp even at the highest dose of 8.3 C/cm^2 that caused T_c to decrease by 11.2 K for $x = 0.32$ sample. Figure 4 summarizes the reduced T_c/T_{c0} obtained from resistivity (open symbols) and penetration depth (full symbols) data plotted versus electron irradiation dose, where T_{c0} is the T_c before irradiation. The variations of T_c/T_{c0} for $x = 0.26$, 0.32, and 0.34 samples were about $\Delta T_c/T_{c0} \simeq$ - 0.04 per C/cm^2, whereas for the most under-doped sample with $x = 0.19$ we find a five times larger value of $\Delta T_c/T_{c0} \simeq$ - 0.2 per C/cm^2. Quantitatively the observed doping dependence of the effect of electron irradiation on T_c is similar to electron-doped $Ba(Fe_{1-x}Co_x)As_2$ [28].

To quantify the evolution of the superconducting gap structure, we analyzed the low temperature part of $\Delta\lambda(T)$ as shown in Fig. 5. The absolute change $\Delta\lambda(T) = \lambda(0.3T/T_c) - \lambda(T_{min}/T_c)$ clearly increases after the irradiation indicating enhanced pair-breaking upon introduction of additional disorder. However, the low temperature $\Delta\lambda(T)$ of the two near-optimally doped samples, 0.32-A and 0.34-B still clearly show exponential saturation below 0.2 T/T_c even after the irradiation. This result suggests that the optimally-doped compositions with isotropic superconducting gaps are extremely robust against electron irradiation, even at the very large dose of 8.3 C/cm^2 which caused suppression of T_c by 11.2 K or $\Delta T_c \approx 0.3T_{c0}$. The situation is similar in a slightly under-doped sample at $x = 0.26$ in which the low temperature saturation is seen below 0.1 T/T_c. In a stark contrast, in the most under-doped sample with $x = 0.19$, where superconductivity and magnetism coexist, the saturating behaviour disappears after the irradiation.

These observations become more apparent when the low-temperature $\Delta\lambda(T)$ is fitted using a power-law function, $\Delta\lambda = A(T/T_c)^n$. The results are plotted in Fig. 5 (e-h). To eliminate the uncertainty related to the upper fitting limit, we performed several fitting runs with a variable high-temperature end of the fitting range, T_{up}/T_c, from 0.1 to 0.3, while keeping the lower limit at the base temperature. The strong saturation behavior of the higher-doping samples is apparent from the large exponent values, $n > 3$, even for the very large irradiation dose of 8.3 C/cm^2. For $x = 0.26$ sample, n increases as the T_{up}/T_c decreases. This implies that the gap remains nodeless, but develops anisotropy with a minimum value about two times smaller than in the cases of a $x = 0.32$ and 0.34 samples. For the most under-doped sample, $x = 0.19$, there is a clear evolution toward the dirty T^2 limit. In the pristine state, the exponent n varied from $n \approx 2.3$ at the widest range to 2.6 - 2.8 at the narrowest T_{up}/T_c range. However, after the irradiation, this tendency reverses. As the T_{up}/T_c decreases, n starts to decrease toward $n = 2$. This is clearly shown in Fig. 6

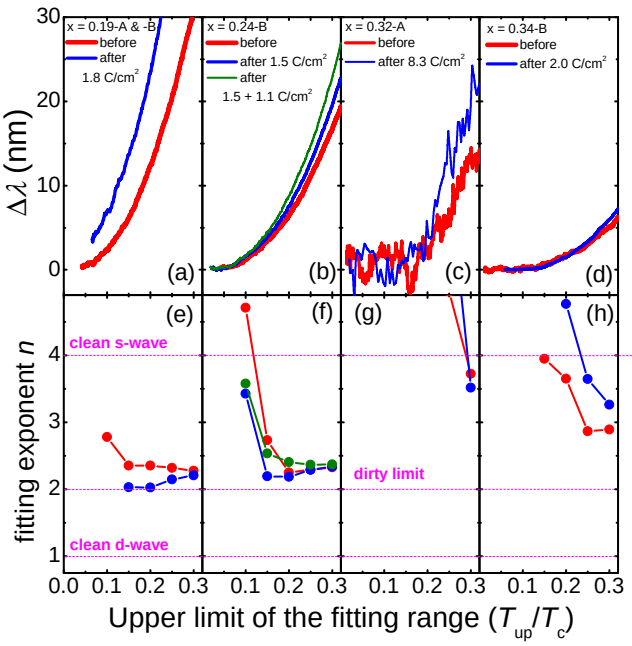

FIG. 5. (Color online) The low temperature part of $\Delta\lambda(T)$ before and after electron irradiation of sample (a) $x = 0.19$, (b) $x = 0.26$, (c) $x = 0.32$, and (d) $x = 0.34$. The data were analyzed with a power-law function, $\Delta\lambda = A(T/T_c)^n$, over a variable temperature range from base temperature to a temperature T_{up}. The corresponding fit exponents are summarized in the bottom raw of panels (e-h). The fitting errors are less than $\pm$ 0.1.

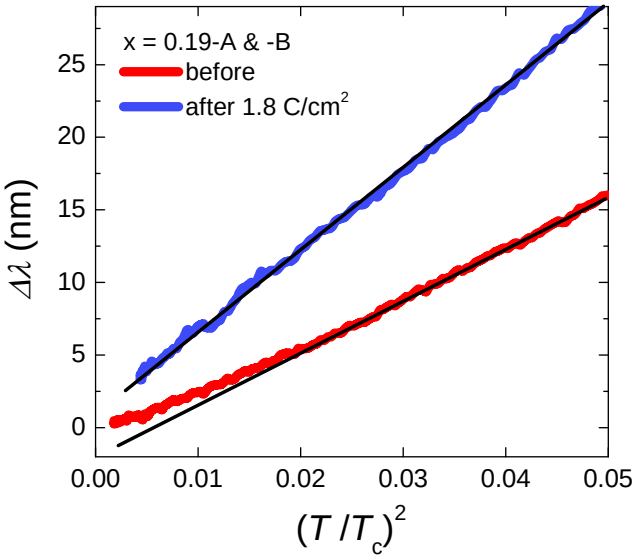

FIG. 6. (Color online) The low temperature part of $\Delta\lambda$ of sample $x = 0.19$ before and after electron irradiation plotted as a function of $(T/T_c)^2$. The straight lines are the guides for the pure T^2 behavior.

where $\Delta\lambda$ is plotted vs. $(T/T_c)^2$. While the data before the irradiation show an upward deviation from T^2, the post-irradiated curve is a clean T^2 line.

Another way to analyze the data is to compare the normalized superfluid density, $\rho_s(T) = \lambda^2(0)/\lambda^2(T)$. Figure 7 shows $\rho_s(T)$ before and after electron irradiation. Since the values of $\lambda(0)$ are not known, we first used the literature value of $\lambda(0) = 200$ nm found for unirradiated optimally doped samples, $x = 0.34$[50–53]. Then, we used the Homes scaling, $\lambda(0) \propto \rho(T_c)/T_c$[49]. Here $\rho(T_c)$ is the resistivity at T_c. The estimated values are $\lambda(0) = 226$ nm and 356 nm for $x = 0.26$ ($T_c = 24.3$ K) and $x = 0.19$ ($T_c = 13.2$ K) samples, respectively. In addition, the maximum possible increase of $\lambda(0)$ induced by the irradiation was estimated by correlating the change of T_c with the pair-breaking scattering and relating it to the expected change of $\lambda(0)$[33]. For example, for $x = 0.32$-A sample, ΔT_c = - 11.2 K after 8.3 C/cm^2 irradiation, so the estimate of $\lambda(0)$ is about 238 nm. Following these two-step procedures, we estimated doping and irradiation dependence of $\lambda(0)$. All values are shown in the labels of Fig. 7.

The superfluid density, $\rho_s(T/T_c)$, is compared in Fig.7 and it is quite different for samples with different x. For near optimally-doped sample with $x = 0.34$, panels (d), the overall behavior follows the expectations for an $s-$wave type pairing. Despite the change of T_c, the irradiation did not change the functional form of $\rho_s(T/T_c)$ much. As the composition moves toward under-doped side ($x = 0.32$ and 0.26 samples), the region of saturation shrinks, but still exists at the lowest temperatures, below 0.2 T/T_c ($x = 0.32$) and 0.1 T/T_c ($x = 0.26$). This small saturation region remains almost intact upon high irradiation of 8.3 C/cm^2 ($x = 0.32$) and 2.6 C/cm^2 ($x = 0.26$) irradiations. In contrast, the superfluid density shows the largest change in the most under-doped sample, $x = 0.19$, where even minor signs of saturation in the pre-irradiated sample disappear after the irradiation. This suggests that the superconducting gap is very anisotropic in heavily under-doped samples and, therefore, is most susceptible to the defects induced by electron irradiation. This result is also consistent with the observation that the largest T_c suppression is found in the most under-doped sample, see Fig. 4. Overall, the full temperature-range shape of $\rho_s(T)$ is close to a full gap $s-$wave behavior in the optimally doped sample and to a line-nodal curve for the most under-doped sample, $x = 0.19$.

IV. CONCLUSIONS

To summarize, the effects of electron irradiation on the in-plane resistivity and London penetration depth were studied in single crystals of hole-doped $(Ba_{1-x},K_x)Fe_2As_2$ superconductor. The irradiation leads to the suppression of the superconducting T_c and of the temperature of the structural/magnetic transition, T_{sm}. The suppression of T_c is much more rapid in the under-doped sample with $x = 0.19$, in which supercon-

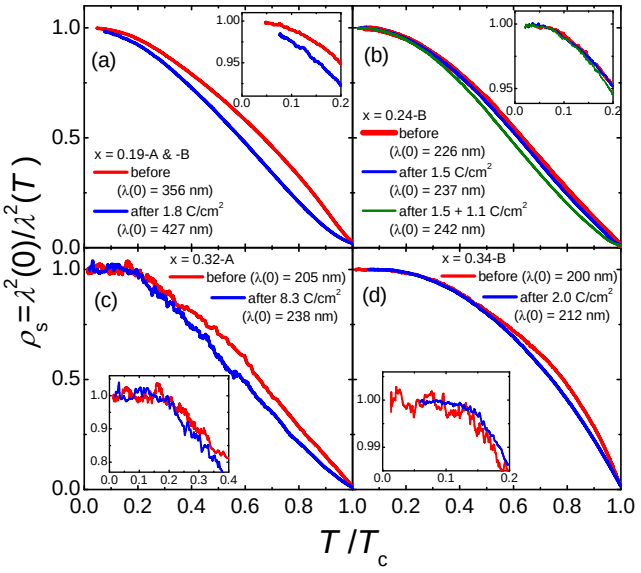

FIG. 7. (Color online) Normalized superfluid density, $\rho_s = (\lambda(0)/\lambda(T))^2$, before and after electron irradiation: for (a) $x = 0.19$, (b) $x = 0.26$, (c) $x = 0.32$, and (d) $x = 0.34$. Doping dependent $\lambda(0)$ was estimated considering resistivity right above T_c (Homes scaling) and irradiation-induced T_c decrease, see text for details.

ductivity coexists with the long range magnetic order. This is consistent with the development of significant gap anisotropy in the coexisting phase. In the coexisting phase, the irradiation might even induce gapless superconductivity. Considering our previous study[36] and the prediction for the rate of suppression of T_c in the extended $s_\pm$ model[6], we suggest that the interband to the intraband pairing ratio increases when moving away from the optimal concentration.

V. ACKNOWLEDGMENTS

We thank A. Chubukov, P. Hirschfeld, V. Mishra and T. Shibauchi for useful discussions. This work was supported by the U.S. Department of Energy (DOE), Office of Science, Basic Energy Sciences, Materials Science and Engineering Division. Ames Laboratory is operated for the U.S. DOE by Iowa State University under contract DE-AC02-07CH11358. We thank the SIRIUS team, B. Boizot, V. Metayer, and J. Losco, for running electron irradiation at *Ecole Polytechnique* (supported by EMIR network, proposal 11-11-0121.) Work in China was supported by the Ministry of Science and Technology of China, project 2011CBA00102.

* Corresponding author: prozorov@ameslab.gov

[1] P. W. Anderson, J Phys Chem Solids **11**, 26 (1959).

[2] A. A. Abrikosov and L. P. Gor'kov, Zh. Eksp. Teor. Fiz. [Sov. Phys. JETP 12, 1243 (1961)] **39**, 1781 (1960).

[3] P. J. Hirschfeld and N. Goldenfeld, Phys. Rev. B **48**, 4219 (1993).

[4] H. Kim, G. Preosti, and P. Muzikar, Phys. Rev. B **49**, 3544 (1994).

[5] A. V. Balatsky, I. Vekhter, and J.-X. Zhu, Rev. Mod. Phys. **78**, 373 (2006).

[6] Y. Wang, A. Kreisel, P. J. Hirschfeld, and V. Mishra, Phys. Rev. B **87**, 094504 (2013).

[7] R. Prozorov, M. Koczykowski, M. A. Tanatar, A. Thaler, S. L. Bud'ko, P. C. Canfield, V. Mishra, and P. J. Hirschfeld, arXiv:1405.3255 (2014).

[8] Y. Mizukami, M. Konczykowski, Y. Kawamoto, S. Kurata, S. Kasahara, K. Hashimoto, V. Mishra, A. Kreisel, Y. Wang, P. J. Hirschfeld, Y. Matsuda, and T. Shibauchi, arXiv:1405.6951 (2014).

[9] G. Xiao, M. Z. Cieplak, J. Q. Xiao, and C. L. Chien, Phys. Rev. B **42**, 8752 (1990).

[10] I. Mazin and J. Schmalian, Physica C **469**, 614 (2009).

[11] P. J. Hirschfeld, M. M. Korshunov, and I. I. Mazin, Rep Prog Phys **74**, 124508 (2011).

[12] A. Chubukov, Ann. Rev. Cond. Matt. Phys. **3**, 13 (2012).

[13] V. Mishra, G. Boyd, S. Graser, T. Maier, P. J. Hirschfeld, and D. J. Scalapino, Phys. Rev. B **79**, 094512 (2009).

[14] A. A. Golubov and I. I. Mazin, Phys. Rev. B **55**, 15146 (1997).

[15] T. Klein, R. Marlaud, C. Marcenat, H. Cercellier, M. Konczykowski, C. J. van der Beek, V. Mosser, H. S. Lee, and S. I. Lee, Phys Rev Lett **105**, 047001 (2010).

[16] Y. Senga and H. Kontani, Journal of the Physical Society of Japan **77**, 113710 (2008).

[17] S. Onari and H. Kontani, Phys Rev Lett **103**, 177001 (2009).

[18] P. Cheng, B. Shen, J. Hu, and H.-H. Wen, Phys. Rev. B **81**, 174529 (2010).

[19] J. Li, Y. Guo, S. Zhang, S. Yu, Y. Tsujimoto, H. Kontani, K. Yamaura, and E. Takayama-Muromachi, Phys. Rev. B **84**, 020513 (2011).

[20] J. Li, Y. F. Guo, S. B. Zhang, J. Yuan, Y. Tsujimoto, X. Wang, C. I. Sathish, Y. Sun, S. Yu, W. Yi, K. Yamaura, E. Takayama-Muromachiu, Y. Shirako, M. Akaogi, and H. Kontani, Phys. Rev. B **85**, 214509 (2012).

[21] H. Kim, R. T. Gordon, M. A. Tanatar, J. Hua, U. Welp, W. K. Kwok, N. Ni, S. L. Bud'ko, P. C. Canfield, A. B. Vorontsov, and R. Prozorov, Phys. Rev. B **82**, 060518 (2010).

[22] C. Tarantini, M. Putti, A. Gurevich, Y. Shen, R. K. Singh, J. M. Rowell, N. Newman, D. C. Larbalestier, P. Cheng, Y. Jia, and H.-H. Wen, Phys Rev Lett **104**, 087002 (2010).

[23] Y. Nakajima, T. Taen, Y. Tsuchiya, T. Tamegai, H. Kitamura, and T. Murakami, Phys. Rev. B **82**, 220504 (2010).

[24] J. Murphy, M. A. Tanatar, H. Kim, W. Kwok, U. Welp, D. Graf, J. S. Brooks, S. L. Bud'ko, P. C. Canfield, and R. Prozorov, Phys. Rev. B **88**, 054514 (2013).

[25] N. W. Salovich, H. Kim, A. K. Ghosh, R. W. Giannetta, W. Kwok, U. Welp, B. Shen, S. Zhu, H.-H. Wen, M. A. Tanatar, and R. Prozorov, Phys. Rev. B **87**, 180502 (2013).

[26] T. Taen, F. Ohtake, H. Akiyama, H. Inoue, Y. Sun, S. Pyon, T. Tamegai, and H. Kitamura, Phys. Rev. B **88**, 224514 (2013).

[27] A. C. Damask and G. J. Dienes, *Point Defects in Metals* (Gordon and Breach Science Publishers Ltd, 1963).

[28] C. J. van der Beek, S. Demirdis, D. Colson, F. Rullier-Albenque, Y. Fasano, T. Shibauchi, Y. Matsuda, S. Kasahara, P. Gierlowski, and M. Konczykowski, Journal of Physics: Conference Series **449**, 012023 (2013).

[29] F. Rullier-Albenque, H. Alloul, and R. Tourbot, Phys Rev Lett **91**, 047001 (2003).

[30] M. Tinkham, *Introduction to Superconductivity*, 2nd ed., Dover Books on Physics (Dover Publications, 2004).

[31] S. K. Yip and J. A. Sauls, Phys Rev Lett **69**, 2264 (1992).

[32] D. Xu, S. K. Yip, and J. A. Sauls, Phys. Rev. B **51**, 16233 (1995).

[33] V. G. Kogan, R. Prozorov, and V. Mishra, Phys. Rev. B **88**, 224508 (2013).

[34] C. P. Strehlow, M. Kończykowski, J. A. Murphy, S. Teknowijoyo, K. Cho, M. A. Tanatar, T. Kobayashi, S. Miyasaka, S. Tajima, and R. Prozorov, Phys. Rev. B **90**, 020508 (2014).

[35] J.-P. Reid, A. Juneau-Fecteau, R. T. Gordon, S. R. de Cotret, N. Doiron-Leyraud, X. G. Luo, H. Shakeripour, J. Chang, M. A. Tanatar, H. Kim, R. Prozorov, T. Saito, H. Fukazawa, Y. Kohori, K. Kihou, C. H. Lee, A. Iyo, H. Eisaki, B. Shen, H.-H. Wen, and L. Taillefer, Superconductor Science and Technology **25**, 084013 (2012).

[36] H. Kim, M. A. Tanatar, W. E. Straszheim, K. Cho, J. Murphy, N. Spyrison, J.-P. Reid, B. Shen, H.-H. Wen, R. M. Fernandes, and R. Prozorov, Phys. Rev. B **90**, 014517 (2014).

[37] H. Fukazawa, Y. Yamada, K. Kondo, T. Saito, Y. Kohori, K. Kuga, Y. Matsumoto, S. Nakatsuji, H. Kito, P. M. Shirage, K. Kihou, N. Takeshita, C.-H. Lee, A. Iyo, and H. Eisaki, Journal of the Physical Society of Japan **78**, 083712 (2009).

[38] K. Okazaki, Y. Ota, Y. Kotani, W. Malaeb, Y. Ishida, T. Shimojima, T. Kiss, S. Watanabe, C.-T. Chen, K. Kihou, C. H. Lee, A. Iyo, H. Eisaki, T. Saito, H. Fukazawa, Y. Kohori, K. Hashimoto, T. Shibauchi, Y. Matsuda, H. Ikeda, H. Miyahara, R. Arita, A. Chainani, and S. Shin, Science **337**, 1314 (2012).

[39] J.-P. Reid, M. A. Tanatar, A. Juneau-Fecteau, R. T. Gordon, S. R. de Cotret, N. Doiron-Leyraud, T. Saito, H. Fukazawa, Y. Kohori, K. Kihou, C. H. Lee, A. Iyo, H. Eisaki, R. Prozorov, and L. Taillefer, Phys. Rev. Lett. **109**, 087001 (2012).

[40] Z. Li, R. Zhou, Y. Liu, D. L. Sun, J. Yang, C. T. Lin, and G.-q. Zheng, Phys. Rev. B **86**, 180501 (2012).

[41] M. A. Tanatar, W. E. Straszheim, H. Kim, J. Murphy, N. Spyrison, E. C. Blomberg, K. Cho, J.-P. Reid, B. Shen, L. Taillefer, H.-H. Wen, and R. Prozorov, Phys. Rev. B **89**, 144514 (2014).

[42] H. Luo, Z. Wang, H. Yang, P. Cheng, X. Zhu, and H.-H. Wen, Supercond. Sci. Technol. **21**, 125014 (2008).

[43] M. A. Tanatar, N. Ni, S. L. Budko, P. C. Canfield, and R. Prozorov, Supercond. Sci. Technol. **23**, 054002 (2010).

[44] R. Prozorov and R. W. Giannetta, Supercond. Sci. Technol. **19**, R41 (2006).

[45] R. Prozorov, R. W. Giannetta, A. Carrington, and F. M. Araujo-Moreira, Phys. Rev. B **62**, 115 (2000).
[46] B. Shen, H. Yang, Z.-S. Wang, F. Han, B. Zeng, L. Shan, C. Ren, and H.-H. Wen, Phys. Rev. B **84**, 184512 (2011).
[47] R. M. Fernandes, M. G. Vavilov, and A. V. Chubukov, Phys. Rev. B **85**, 140512 (2012).
[48] V. G. Kogan, Phys. Rev. B **80**, 214532 (2009).
[49] C. C. Homes, S. V. Dordevic, M. Strongin, D. A. Bonn, R. Liang, W. N. Hardy, S. Komiya, Y. Ando, G. Yu, N. Kaneko, X. Zhao, M. Greven, D. N. Basov, and T. Timusk, Nature **430**, 539 (2004).
[50] C. Martin, R. T. Gordon, M. A. Tanatar, H. Kim, N. Ni, S. L. Bud'ko, P. C. Canfield, H. Luo, H. H. Wen, Z. Wang, A. B. Vorontsov, V. G. Kogan, and R. Prozorov, Phys. Rev. B **80**, 020501 (2009).
[51] C. Ren, Z.-S. Wang, H.-Q. Luo, H. Yang, L. Shan, and H.-H. Wen, Phys Rev Lett **101**, 257006 (2008).
[52] G. Li, W. Z. Hu, J. Dong, Z. Li, P. Zheng, G. F. Chen, J. L. Luo, and N. L. Wang, Phys Rev Lett **101**, 107004 (2008).
[53] D. V. Evtushinsky, D. S. Inosov, V. B. Zabolotnyy, M. S. Viazovska, R. Khasanov, A. Amato, H.-H. Klauss, H. Luetkens, C. Niedermayer, G. L. Sun, V. Hinkov, C. T. Lin, A. Varykhalov, A. Koitzsch, M. Knupfer, B. Buchner, A. A. Kordyuk, and S. V. Borisenko, New J. Phys. **11**, 055069 (2009).